Calibration, correction and flagging from the chlorophyll fluorometer on GoMOOS Buoy A01: November 2005-June 2014

Massachusetts Water Resources Authority
Environmental Quality Department
Report 2014-14

Calibration, Correction and Flagging of Data from the Chlorophyll Fluorometer on GoMOOS Buoy A01: Nov 2005 – Jun 2014

Principal Investigator:	Dr. Collin Roesler
Institution:	Bowdoin College Department of Earth and Oceanographic Science
Address:	6800 College Station Brunswick, ME 04011
Phone/Fax:	207-725-3842 / 207-798-7037
Email:	croesler@bowdoin.edu

Period of Performance: 1 July 2013 - 30 June 2014

Roesler, CS. 2014. Calibration, Correction and Flagging of Data from the Chlorophyll Fluorometer on GoMOOS Buoy A01: Nov 2005 – Jun 2014. Boston: Massachusetts Water Resources Authority. Report 2014-14. 11 p.

Introduction

Thirteen years of real-time hourly observations of hydrographic and bio-optical measurements have been collected by the Gulf of Maine Integrated Ocean Observations System (formerly GoMOOS, now NERACOOS). Initially, 4 buoys were equipped with optical sensors (B, E, I, and M; figure 1); Buoy A was instrumented in late 2005 through support from MWRA; Buoy F (Penobscot Bay) through support from NASA, and more recently Buoy D02 (Harpswell Sound) through support from NSF and NASA. Buoy A optical sensors consist of a WETLabs combination chlorophyll fluorometer/turbidity sensor (ECO-series FLNTU) and a DH4 data handler that provides the mean values of 30-second burst sampling each hour to the buoy data logger for real time transmission (http://gyre.umeoce.maine.edu/data/gomoos/buoy/html/A01.html). The time course observations of calibration chlorophyll fluorescence and turbidity at buoy A are presented in this report from the perspective of the sources of variability in determining phytoplankton biomass from *in situ* fluorescence and from the perspective of observing phytoplankton dynamics.

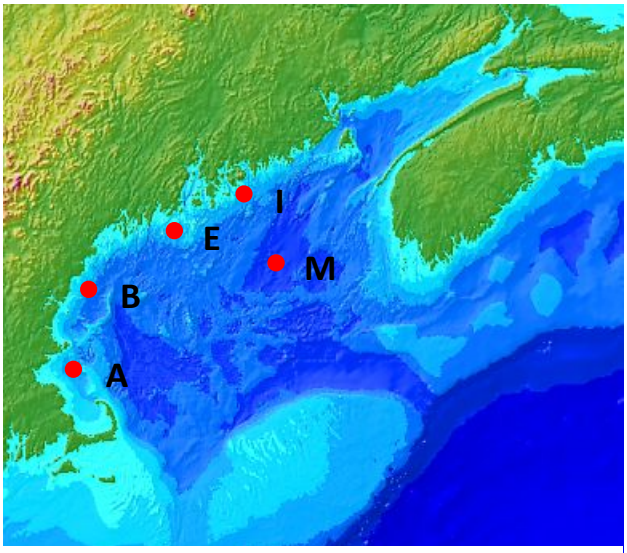

Figure 1. Map of the Gulf of Maine bathymetry (courtesy R. Signell) with the location of opticallyinstrumented shelf and basin buoys are indicated by red symbols.

Methods

The two FLNTU sensors are serviced and calibrated by the WET Labs factory in between each deployment. Additionally, the fluorometers are calibrated in the lab prior to deployment using ten dilutions of a monospecific culture of the diatom *Thalassiosira pseudonana*. The culture is grown in nutrient replete L1 media at an irradiance that maximizes growth rates (i.e. ~300 µEin m^{-2} s^{-1}) and minimizes pigment packaging due to low light acclimation. The culture is harvested in exponential growth with maximal extracted chlorophyll concentrations of 20 to 50 mg m^{-3}. The fluorescence efficiencies of the culture have been shown to be repeatable over years (Proctor, C. W., and C. S. Roesler. 2010). This approach to calibration thus provides not only a consistent calibration between deployments, it also provides a more realistic estimate of *in vivo* chlorophyll concentrations from *in situ* fluorescence than do vicarious, *in-situ* calibration approaches due to the uncertainties in species composition, light and nutrient history and acclimation, degree of non-photochemical quenching and detrital pigment fluorescence.

Our laboratory calibrations are typically performed during mid-day hours (for consistency in cell physiology) on *T. pseudonana* populations temporarily held in low light so the cells are not affected by non-photochemical quenching. The cells under culture do undergo some level of non-photochemical quenching as do phytoplankton *in situ*. Typical variations in fluorescence

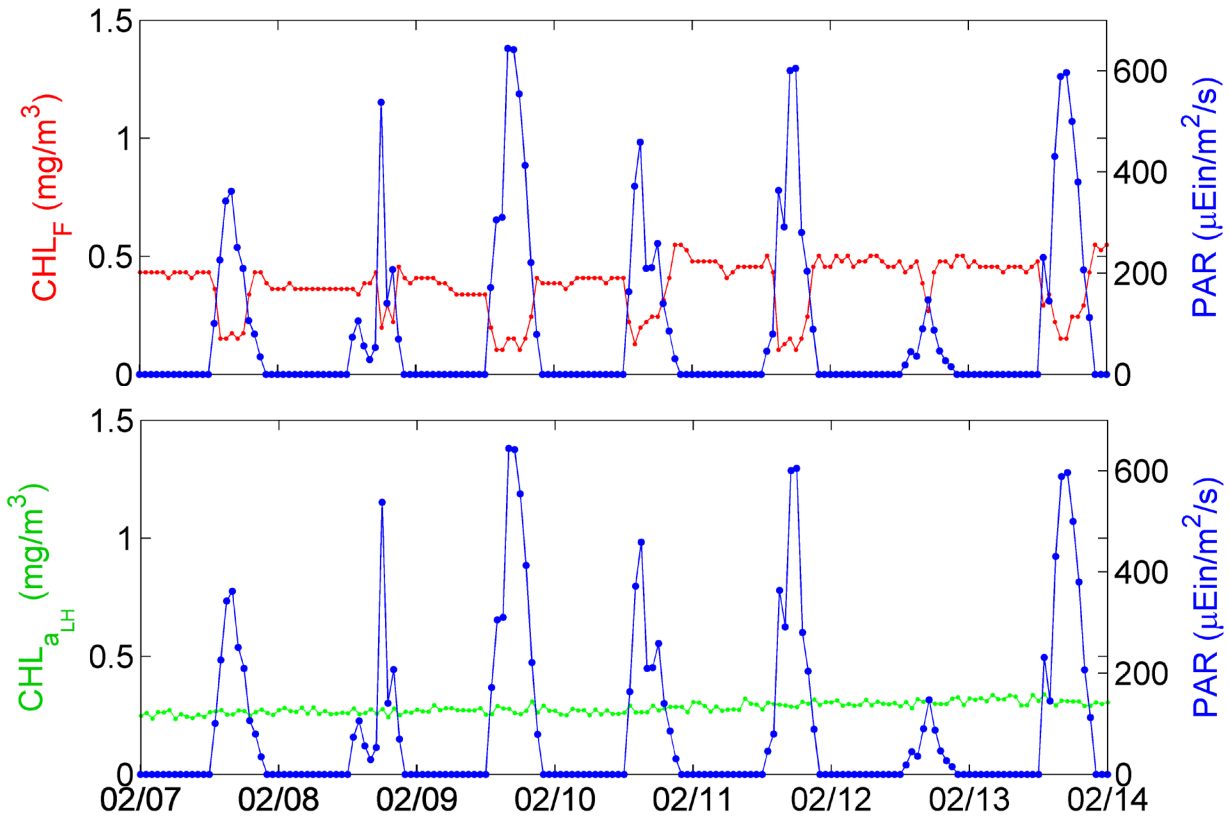

Figure 2. Time series of hourly observations from GoMOOS buoy I in February 2009. Photosynthetically Available Radiation (PAR) is shown in blue in both panels. Calibrated chlorophyll fluorescence is shown in red in top panel, calibrated chlorophyll absorption (which is not impacted by non-photochemical quenching) is shown in green in bottom panel. The calibrated chlorophyll absorption is computed from the absorption line height of the red chlorophyll absorption peak measured by an *in situ* absorption meter (WET Labs, ac9) and scaled by the chlorophyll-specific absorption coefficient derived from field and culture samples (Roesler, C. S., and A. H. Barnard. 2013).

yield (fluorescence per unit chlorophyll) are of order factor of 2 but can reach an order of magnitude (Figure 2) depending upon the intensity of ambient light. Daytime surface readings of chlorophyll fluorescence can therefore underestimate chlorophyll concentration by more than a factor of two. In the absence of other optical sensors, night time observations are likely the most robust estimates of chlorophyll concentration from *in situ* fluorometers. The *in situ* fluorescence yield (*in situ* chlorophyll fluorescence to chlorophyll concentration ratio) is found to decrease as PAR increases above 100 µEin m^{-2} s^{-1} (Figure 3) due to non-photochemical quenching, reaching minimal values above about 300 µEin m^{-2} s^{-1}. These irradiance levels are consistent with mid-morning conditions in near surface waters on cloud-free days and may extend to the upper 10m to 20m depths in the Gulf of Maine depending upon the local water clarity.

Laboratory calibrations thus provide internal consistency so that temporal variations can be quantitatively interpreted. To achieve robust and accurate estimates of chlorophyll

concentration in the field, it is best to do point-by-point *in situ* validation with samples that are collected before 0900 hours in the day, when non-photochemical quenching of the fluorometer is minimized. Another approach is to use an absorption meter paired with a fluorometer; this approach provides accurate chlorophyll concentration and additionally the photosynthetic parameter, E_k, describing the half saturation coefficient for photosynthesis necessary for bio-optical modeling of photosynthesis, and a qualitative assessment of phytoplankton taxonomy (Roesler, C. S., and A. H. Barnard 2013).

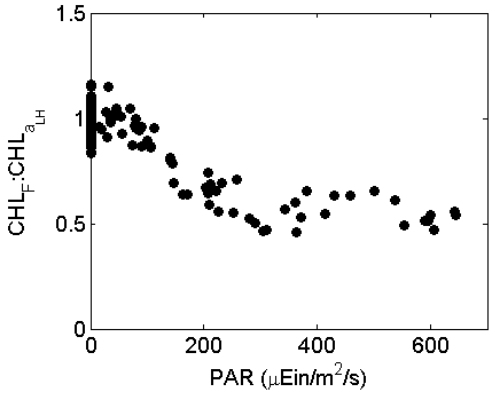

Figure 3. Hourly observations of the *in situ* fluorescence yield versus instantaneous PAR, from the time series shown in Figure 2. From Roesler and Barnard 2013.

Drift and biofouling are assessed in two ways. Instrumental drift is quantified as the difference in dark reading before and after each deployment. Over the lifetime of the sensors, sensor drift over the duration of the deployments has been negligible compared to the scale of natural variations observed in the fluorescence signal (Figure 4). Instrument drift is assessed upon sensor recovery in the laboratory as one for which the dark current is significantly different compared to that determined at the start of the deployment. Sensors drift tends to manifest itself in the realtime data as a long-term trend that is removed once the endpoint dark values are determined. It may also appear as a step change rather than a slowly evolving trend. Regardless, endpoint dark reading combined with evaluation of the *in situ* time series are used to identify drift (Roesler, C. S., and E. Boss 2008). Biofouling appears to be the dominant factor leading to uncertainties in the observed fluorescence and turbidity signals on Buoy A. Biofouling is typically observed towards the end of each deployment interval and is quantified by the difference in calibrated observations collected on the last day of a deployment and the first day of the subsequent deployment (Figure 5), although the patterns of biofouling have distinct features.

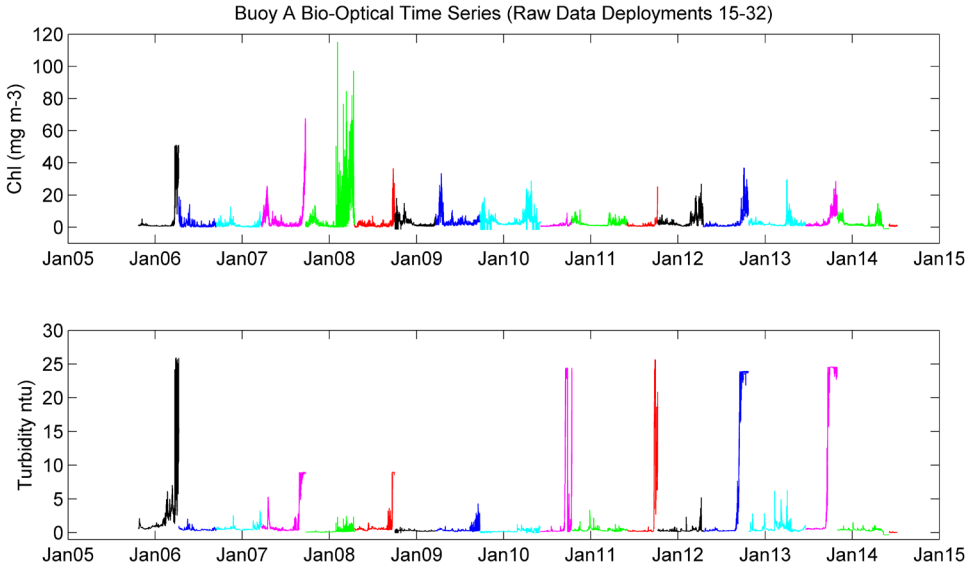

Figure 4. Time series of real time observations of calibrated chlorophyll fluorescence (top panel) and turbidity (bottom panel) color-coded by deployment (deployments 15-32).

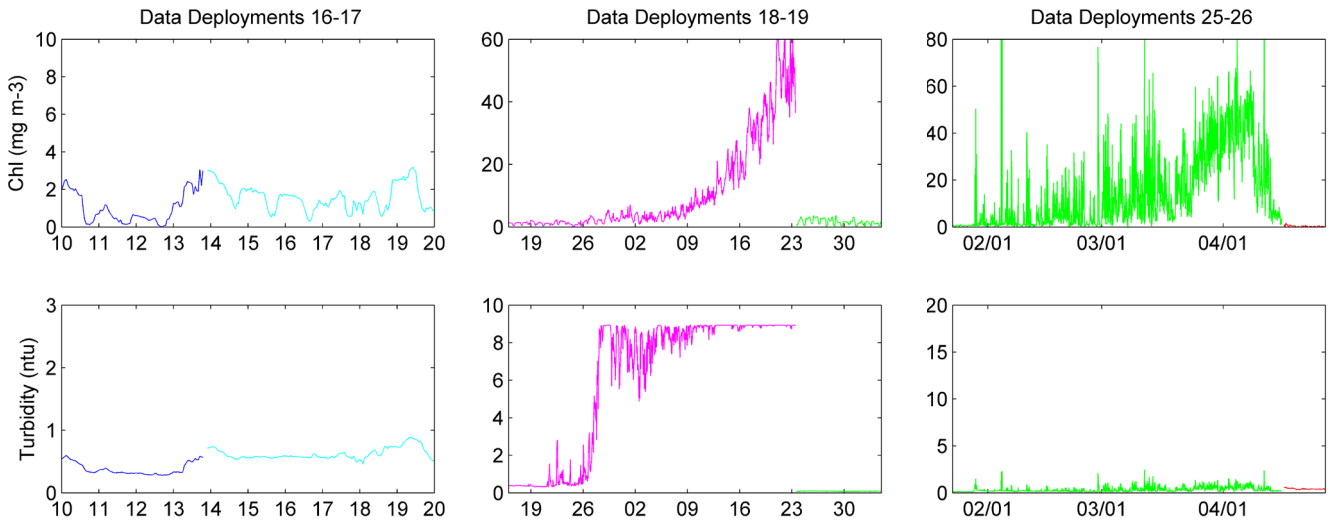

Figure 5. Three examples of deployment-to-deployment transitions in chlorophyll fluorescence and turbidity to assess biofouling: (*left*) 16 to 17, (*middle*) 18 to 19, (*right*) 25 to 26, showing negligible biofouling, saturated biofilm, and frondular biofouling, respectively.

For example, there may be no quantitative differences in the bio-optical signatures between deployments (Figure 5, *left panels*) indicating that there is no biofouling, there was not instrument drift, and the instrument calibrations performed pre-deployment were robust. This type of transition between deployments occurred 7 times out of the 17 deployments.

A second pattern observed in the deployment transition is one of biofilm-type biofouling in which the optical windows become increasingly covered with a bio-film which results in an exponentially increasing fluorescence and/or turbidity signal (Figure 5 *center panels*), although the rate of biofouling will be different for the two signals. In these situations, the data are not recoverable and thus are flagged and removed from the time series.

Figure 6. Example of extreme frondular biofouling by colonial hydroid polyps on the ECO FLNTU observed upon recovery of deployment 30. *Photo credit M. Mickelson.*

The third pattern, “frondular biofouling”, observed in the deployment transition is biofouling by larger organisms (Figure 5 *right panels*, particularly chlorophyll signal) such as seaweeds or sessile invertebrates, which grow on the sensors or frame (Figure 6) and waft into the sensing volume. This results in highly variable and enhanced signals in fluorescence and/or turbidity. Because this type of biofouling does not coat the sensor optical window, it may be possible to recover a robust fluorescence and turbidity sensor by re-analysis of the burst sampling data. Presumably there would be some observations in the burst sampling for which there was no contamination by the wafting biota and thus perhaps computing the minimum of each burst sample might provide the estimate of the bio-optical

signal of the seawater in absence of biofouling. This approach is currently being investigated.

Figure 7 shows the full time series of hourly observations of fluorescence and turbidity with data points flagged to indicate biofouling, drift or offset and anomalous negative values (green, red and blue data points, respectively. Notice that there is not necessarily a coherence between the two signals because of how bio-films and frondular growth differently impact fluorescence and turbidity. Negative values occur when the raw observations are less than dark readings. These rare occurrences are found either as errors in data communication between sensors and data loggers, associated with variability in dark values (signal to noise at the level of dark readings) or when frondular biofouling impedes the sampling volume such that raw observations approach dark readings. Thus, when calibration factors are applied to the raw digital counts, values are slightly negative. On rare occasions deployment-to-deployment offsets are observed. These are indicated by offsets from both the prior and post deployments and indicate an error in the calibration coefficients. These occurrences are identified in the real time data and are corrected in the post-processing analyses by re-analysis of the pre- and post-deployment sensor calibrations.

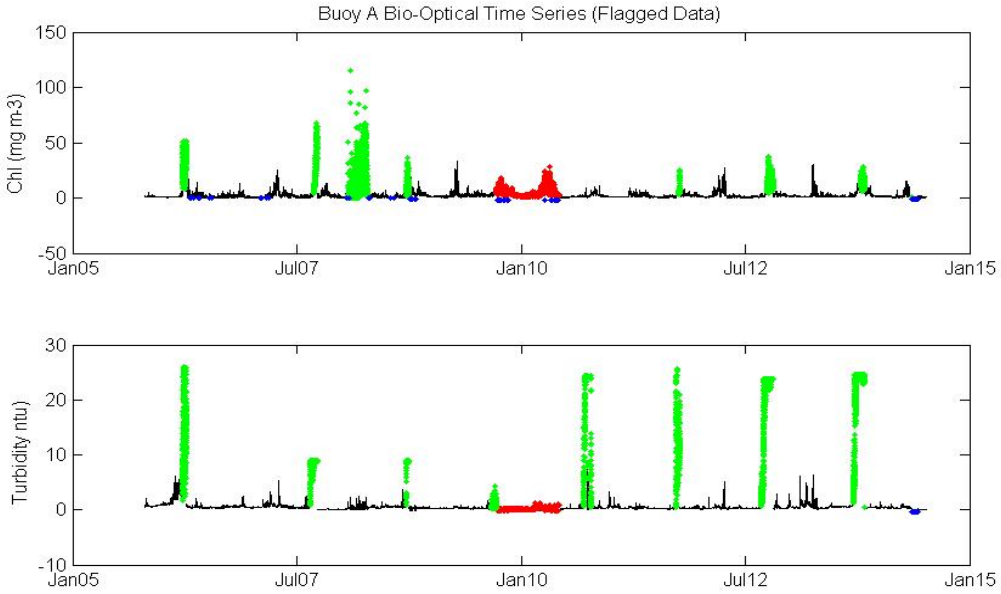

Figure 7. Hourly observations of calibrated chlorophyll fluorescence and turbidity color coded by flagged data: biofouling (green), deployment-to-deployment offsets (red) and negative values (blue).

The submitted data file of hourly observations is now provided in the following format:
BuoyA_2014_optics.dat =
[Year Month Day Hour Minute Second Chl_clean Chl_raw Flag_CHL NTU_clean NTU_raw Flag_NTU]

where the _clean columns are those for which the negative values and biofouling-impacted observations have been removed and the sensor offset values corrected; the Flag_ columns are coded to indicate good values (0), anomalous values below zero removed (1), values removed due to biofouling (2), values corrected for sensor offsets (3).

Results

The QA/QC data set of hourly observations is presented in Figure 8. There is still a lot of variability observed but there is no concrete evidence for a need for further correction of the data (e.g. there appears to be higher background turbidity in early deployments of 2006 but there is no reliable connection to correct the offset between deployments because there was no post calibration performed on the sensor at the time. Additional offset correction would be guessing and without statistical merit.

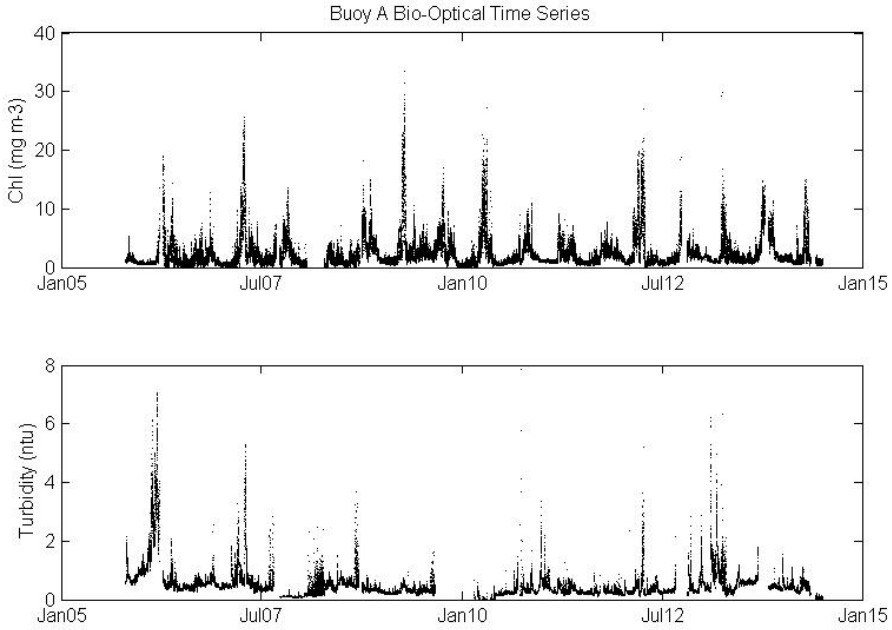

Figure 8. Hourly observations of calibrated chlorophyll fluorescence and turbidity with flagged observations removed, offsets corrected.

The hourly chlorophyll fluorescence does still contain the depressed observations due to non-photochemical quenching. Daily values are computed for more reliable analysis of biomass (Figure 9). The format of the data file is:

BuoyA_2014_optics_daily.dat =
[Year Month Day Chl_median Chl_std Chl_Flagmax NTU_median NTU_std NTU_Flagmax]

where median and standard deviations are computed over each day (excepting the high light region of the day, 0900 to 1500), and Flagmax is the maximum flag number observed at least once in that day (indicating the potential correction for that day).

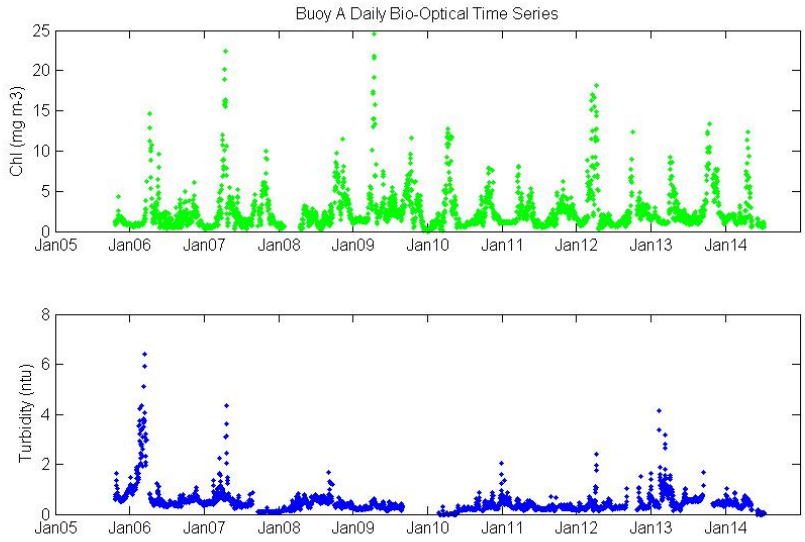

Figure 9. Daily median observations of calibrated chlorophyll fluorescence and turbidity.

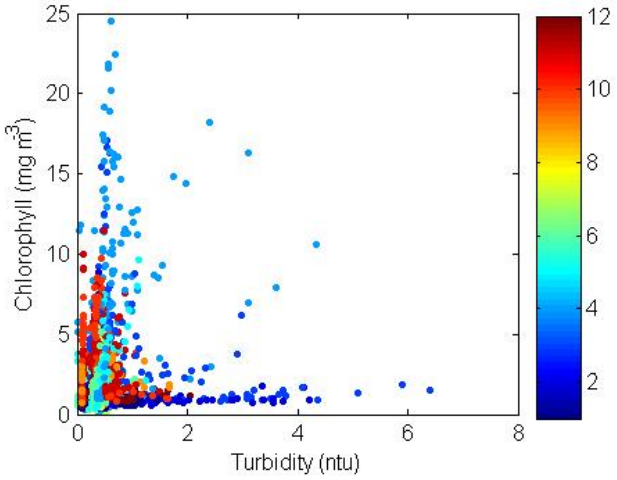

Figure 10. Relationship between daily chlorophyll and turbidity observations (from Figure 5) color coded by month.

There is a bimodal pattern in the relationship between phytoplankton biomass (as estimated by chlorophyll fluorescence) and total suspended particulate mass (as estimated from turbidity). When phytoplankton blooms develop, there is a weak but linear increase in the turbidity (as evidenced by the data cloud with a steep slope) (Figure 10). This suggests that phytoplankton cells contribute weakly to the particle backscattering and hence turbidity signal, as has been suggested by Ulloa et al. (1994) due to their high absorption to backscattering ratios. In contrast, during early winter months (January to February), the high turbidity values are observed during times of negligible phytoplankton concentrations. This high suspended particular load may be associated with river-borne material transported during spring freshet.

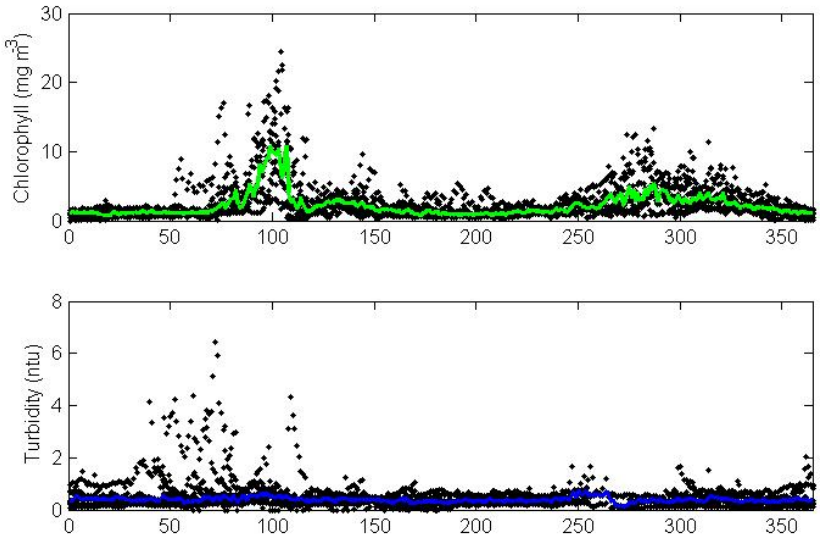

Figure 11. Annual climatology for chlorophyll and turbidity computed from the daily median values 2005-2014.

The annual climatology of daily chlorophyll and turbidity observations (Figure 11) indicates an intense spring bloom of magnitude 10 (mg chl m^{-3}) peaking on April 10, with a duration of order three weeks. The fall bloom is of order 5 (mg chl m^{-3}), peaks late September but last a few months climatologically. Within any particular year, however, the spring bloom can peak as early as mid-February (e.g. 2012) or as late as April 20 (e.g. 2014) with peak values below 10 (mg chl m^{-3}, 2011 and 2013) or in excess of 20 (mg chl m^{-3}, 2007 and 2009). The fall blooms can be non-existent (e.g. 2006) or can exhibit multiple peaks (e.g. 2008). There is virtually no seasonal climatology in turbidity although year-to-year features are observed, particularly in the late winter early spring. This time interval is associated with the spring freshet with maximal river discharge and likely covarying increases in suspended sediment that would have a large turbidity signature but minimal chlorophyll signal.

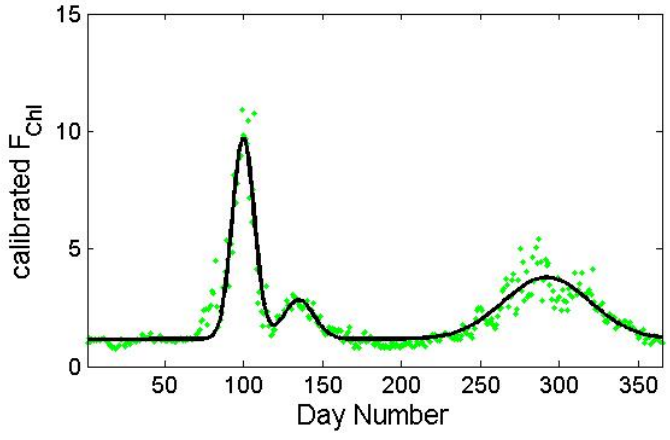

Figure 12. Daily climatological observations of chlorophyll fluorescence as shown in Figure 11 (green) and best fit Gaussian model (black). The values for the Gaussians are provided in Table 1. The background chlorophyll concentration was 1.2 mg m^{-3}.

The climatological spring and fall phytoplankton blooms are fit to a series of Gaussian functions so as to estimate an analytic model for the climatology (Figure 12). The climatology, as well as the year-to-year patterns in spring blooms, indicate the occurrence of two spring blooms; a larger bloom

centered on day 100 and a second smaller peak centered on day 130. The statistical estimates of the best fit model parameters are provided in Table 1.

Table 1. Statistical estimates of bloom parameters for Gaussian model of climatology.

	First Spring Bloom	Second Spring Bloom	Fall Bloom
Amplitude (mg m^{-3})	8.5	2.6	1.6
Date of Peak (d)	99.7	134.9	291.9
Duration (d)	6.9	9.7	27.3

Climatologically, the magnitude of the spring bloom exceeds that of the fall bloom, while the duration is much shorter. This pattern was not observed in 2013 (Figure 13); the peak value of the spring bloom was below average and was lower than the peak value of the fall bloom. The secondary spring bloom was not observed. Bloom timing was climatologically typical.

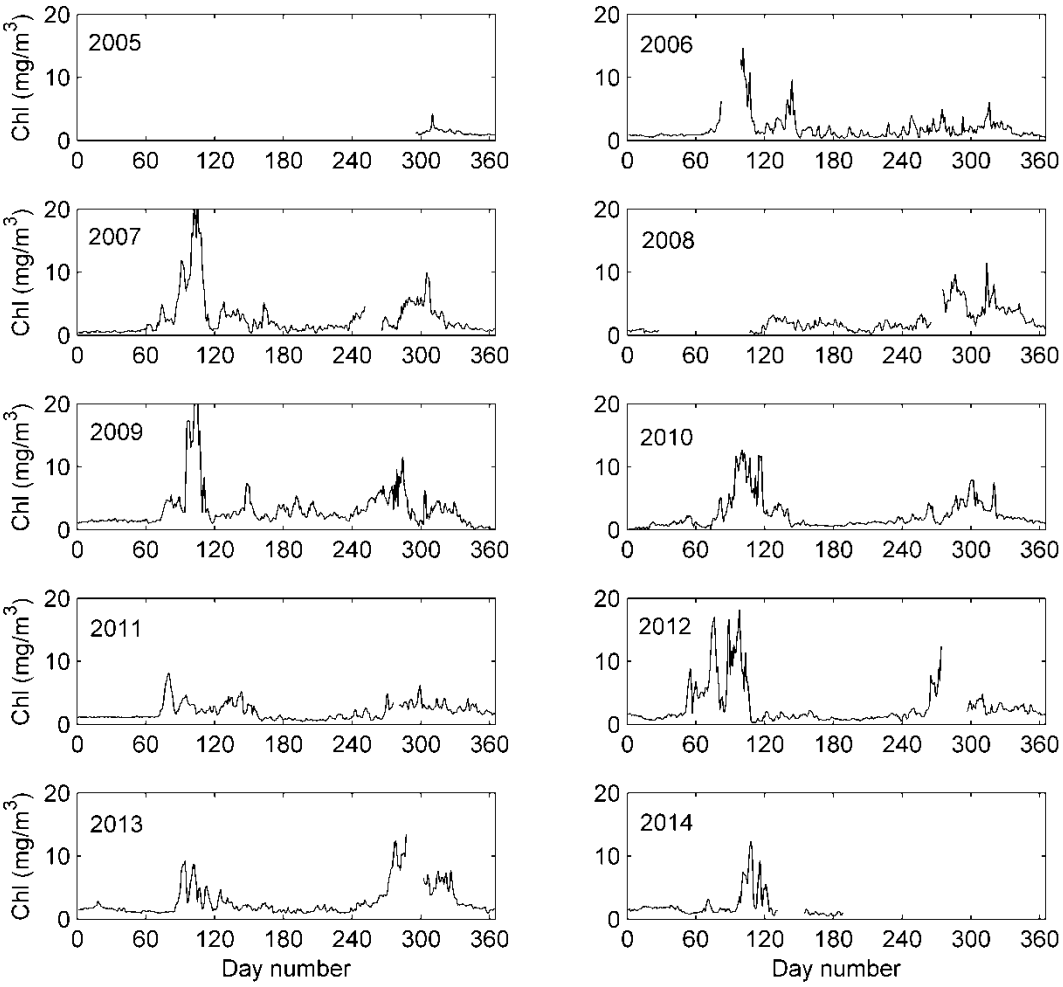

Figure 13. Daily chlorophyll time series for each year of observations, showing year-to-year variations. 2013 was notable in the relative magnitudes of the spring and fall blooms, with fall bloom concentrations exceeding those in the spring. The timing of the blooms was typical.

Summary

Over eight years of hourly bio-optical observations of calibrated chlorophyll fluorescence and turbidity collected from the NERACOOS Buoy A has undergone post-processing. Three flags have been applied to the data to indicate instrumental offset (dark reading) corrections, anomalous negative readings (after offset corrections), and biofouling impacted data. The latter was separated into two types of biofouling, biofilm versus frondular growth. Both were removed from the data. We are investigating two strategies for optimized correction of each type of biofouling and will be reporting on it in the coming year.

The hourly fluorescence observations are impacted by non-photochemical quenching and thus daily observations are more robust. The seasonal climatology for buoy A suggests two main blooms, spring and fall, with a small late spring bloom evident more than half of the sampled years. There is no climatological pattern evident in turbidity but appears to more linked to the spring freshet. The daily observation of chlorophyll for 2013 suggests a smaller than expected spring bloom with peak values less than those observed in the fall. This pattern has not been observed in other years.

References

Proctor, C. W., and C. S. Roesler. 2010. New insights on obtaining phytoplankton concentration and composition from *in situ* multispectral Chlorophyll fluorescence. Limnology and Oceanography: Methods 8**:** 695-708.

Roesler, C. S., and A. H. Barnard. 2013. Optical proxy for phytoplankton biomass in the absence of photophysiology: Rethinking the absorption line height. Methods in Oceanography 7: 79-94.

Roesler, C. S., and E. Boss. 2008. *In situ* measurement of the inherent optical properties (IOPs) and potential for harmful algal bloom (HAB) detection and coastal ecosystem observations., p. 153-206. *In* M. Babin, C. S. Roesler and J. C. Cullen [eds.], *Real-time Coastal Observing Systems for Marine Ecosystem Dynamics and Harmful Algal Blooms: Theory, Instrumentation and Modelling*. UNESCO.

Ulloa, O., S. Sathyendranath, and T. Platt. 1994. Effect of the particle-size distribution on the backscattering ratio in seawater. Applied optics **33:** 7070-7077.

Massachusetts Water Resources Authority
Charlestown Navy Yard
100 First Avenue
Boston, MA 02129
(617) 242-6000
www.mwra.com